The First Human Application of an F-18-labeled Tryptophan Analog for PET Imaging of Cancer

Otto Muzik (otto@pet.wayne.edu)
Wayne State University https://orcid.org/0000-0002-5483-4452
Anthony F. Shields
Wayne State University School of Medicine
Geoffrey R. Barger
Wayne State University School of Medicine
Huailei Jiang
Wayne State University School of Medicine
Parthasarathi Chamiraju
Wayne State University School of Medicine
Csaba Juhász
Wayne State University School of Medicine

Research Article

Keywords: fluorine-18-labeled tryptophan analog, radioactive tracer, tryptophan metabolism, kynurenine pathway, indoleamine 2,3-dioxygenase, PET, molecular imaging

Posted Date: September 25th, 2023

DOI: https://doi.org/10.21203/rs.3.rs-3355828/v1

Version of Record: A version of this preprint was published at Molecular Imaging and Biology on November 27th, 2023. See the published version at https://doi.org/10.1007/s11307-023-01877-8.

Abstract

Purpose. Preclinical studies showed the tryptophan analog PET radiotracer 1-(2-^{18}F-fluoroethyl)-L-tryptophan (^{18}F-FETrp) to accumulate in various tumors, including gliomas, and being metabolized via the immunosuppressive kynurenine pathway. In this first-in-human study, we tested the use ^{18}F-FETrp-PET in patients with neuroendocrine and brain tumors.

Procedures. We applied dynamic brain imaging in patients with gliomas (n = 2) and multi-pass 3D whole-body PET scans in patients with neuroendocrine tumors (n =4). Semiquantitative analysis of organ and tumor tracer uptake was performed using standardized uptake values (SUVs). In addition, organ dosimetry was performed based on extracted time-activity curves and the OLINDA software.

Results. Neuroendocrine tumors showed an early peak (10-min post-injection) followed by washout. Both gliomas showed prolonged ^{18}F-FETrp accumulation plateauing around 40-min and showing heterogeneous uptake including non-enhancing tumor regions. Biodistribution showed moderate liver uptake and fast clearance of radioactivity into the urinary bladder; the estimated effective doses were similar to other ^{18}F-labeled radioligands.

Conclusions. The study provides proof-of-principle data for the safety and potential clinical value of ^{18}F-FETrp-PET for molecular imaging of human gliomas.

INTRODUCTION

Tryptophan is an essential amino acid required for biosynthesis of proteins, serotonin, and niacin [1]. Under some pathologic conditions, including cancers, induction of indoleamine 2,3-dioxygenase (IDO) also leads to increased tryptophan metabolism via the kynurenine pathway (KP) that can exert a strong immunosuppressive effect [2, 3]. Pharmacological blockade of KP activity can reverse this immune suppression [2–4]. Human studies using molecular imaging targeting tryptophan metabolism may clarify the role of tryptophan metabolism in the biological behavior of malignant tumors and identify tumors likely to respond to KP inhibition.

We have previously used alpha-[^{11}C]-methyl-L-tryptophan (^{11}C-AMT) in human cancer imaging with positron emission tomography (PET) [5–9]. ^{11}C-AMT can be metabolized to serotonin, and, to a certain degree, via the KP [10] and has shown several potential neuro-oncology applications [5, 7–9]. However, the clinical use of ^{11}C-AMT-PET is limited due to the radiotracer's short half-life, cumbersome radiosynthesis, and its reflection of multiple metabolic pathways. Here we report the first human experience with the ^{18}F-labeled tryptophan analog 1-(2-[^{18}F]fluoroethyl)-L-tryptophan (^{18}F-FETrp). Preclinical studies showed ^{18}F-FETrp to be the substrate of IDO [11–15]. Here we applied ^{18}F-FETrp-PET to establish its safety and potential utility to image human gliomas known to express IDO [16]. We also scanned patients with neuroendocrine tumors that can upregulate the serotonin (but not the kynurenine)

pathway and were expected to show lower ^{18}F-FETrp accumulation, while allowing body imaging to evaluate the tracer's biodistribution and perform dosimetry.

METHODS

Subjects. Six patients (4 females, age: 56 ± 10 years, body weight: 81 ± 18 kg) participated in this study. Four had previously diagnosed neuroendocrine tumors, and the remaining two had a brain tumor, glioma on subsequent histopathology. Inclusion/exclusion criteria are given in Supplemental Data. The subjects' vital signs were recorded before radioligand injection and at the conclusion of the PET scan (~ 70 min p.i.). The study was approved by the WSU Institutional Review Board, and all participants signed a consent form.

Radioligand preparation. ^{18}F-FETrp was prepared as described recently [17] and was carried as outlined in our FDA-approved Investigational New Drug Application (#162,122). ^{18}F-FETrp was obtained with high radiochemical purity (> 99%) and had specific radioactivity of 226 ± 19 GBq/μmol (N = 6 batches) at the time of injection. The mean and standard deviation of the administered mass of ^{18}F-FETrp was 0.78 ± 0.40 ug (range, 0.35–1.50 μg). The mean administered activity was 470 ± 140 MBq (300–630 MBq). There were no adverse or clinically detectable pharmacologic effects in any subjects, and no significant changes in vital signs or the results of laboratory studies or electrocardiograms were observed.

PET/CT acquisition. All scans were performed using a GE Discovery STE PET/CT scanner (Waukesha, WI, USA). Before tracer injection, a low-dose helical CT (60 mA, 100 kVp) scan was acquired for attenuation correction and localization. Following intravenous injection of ^{18}F-FETrp (5.2 MBq/kg), patients with a brain tumor underwent a 3D dynamic brain scan (5x3, 3x5, 3x10min), whereas patients with neuroendocrine tumors underwent a multi-pass 3D whole-body PET scan (3min/bed) consisting of three sequential acquisitions (0–20, 20–40, 40-60min). Images were reconstructed with OSEM image reconstruction using 28 subsets with 4 iterations and were corrected for attenuation.

Image analysis. For semiquantitative analysis of organ and tumor tracer uptake, standardized uptake values (SUVs) in regions representing various organs/tissues were determined. A complete set of organs was automatically segmented from CT image volumes using the multiple-organ objective segmentation (MOOSE) software [18] (details in Supplemental Data). Tumor regions were defined on PET/CT images co-registered with the subjects' magnetic resonance images (MRIs) or CT images. For the brain tumors, where tracer uptake was heterogeneous within the MRI-defined tumor mass, circular ROIs with a diameter of at least 6 mm were placed manually on the MRI-co-registered PET images centered around the maximum uptake area in two 3-mm axial slices. For the hemispheric tumor, additional ROIs were used in adjacent lower-uptake contrast-enhancing tumor regions.

Calculating residence times. The residence time for each organ was calculated using the OLINDA software [19, 20] (see details in Supplemental Data).

RESULTS

Biodistribution of ^{18}F-FETrp. The urinary bladder had the highest uptake, with a peak of 40% of injected activity at 10-min (Fig. 1). Similar to the kinetics of the bladder, radioactivity peaked in the first image acquisition for the liver (10%), kidneys (5.0%), and other organs and decreased throughout the length of the scan (Fig. 2). The scans showed no significant bone radioactivity.

Dosimetry of ^{18}F-FETrp. The organs with their residence time are listed in **Table 1**. The organ with the highest radiation dose (μGy/MBq) was the urinary bladder wall, followed by the kidneys and liver (**Table 2**). The effective dose equivalent (EDE) was 14.7 μSv/MBq for males and 18.3 μSv/MBq for females. The total patient dose (EDE) for a clinical study, when administering a dose of 5.2 MBq/kg (equivalent to 0.14 mCi/kg), was 5.3 mSv (530 mrem) for males and 5.7 mSv (570 mrem) for females.

Tumor uptake of ^{18}F-FETrp. Both gliomas showed ^{18}F-FETrp accumulation plateauing around 40min after tracer injection (Fig. 3). Tracer uptake in normal brain was low, providing an excellent tumor-to-background contrast. Tracer uptake was heterogeneous in both tumor masses: in the hemispheric glioma, the highest ^{18}F-FETrp-uptake area was confined to a portion of the contrast-enhancing mass (Fig. 3A). Histopathology from this area showed a WHO grade II astrocytoma (IDH1-mutated with gemistocytic features). In the brainstem glioma, high ^{18}F-FETrp uptake encompassed a portion of non-enhancing area with high FLAIR signal (Fig. 3B), which was biopsied and showed a diffuse astrocytoma (Ki-67 6–8%, IDH2-mutated). SUV at 40-60min post-injection in the highest uptake region was 3.5 in the hemispheric and 2.2 in the brainstem glioma, yielding a tumor-to-cortex ratio of ~ 7 and 4.5, respectively. Tracer uptake peaked early in the neuroendocrine tumors and was lower with an average SUV of 2.0 and a tumor to tissue contrast of ~ 2:1 (Fig. 4).

DISCUSSION

This first human PET study with ^{18}F-FETrp, a tryptophan analog with the potential to evaluate tumoral tryptophan transport and metabolism via the KP demonstrates the safety and biodistribution of this radiotracer, with a fast ^{18}F-FETrp excretion into the urinary bladder, with small residual activity in the liver and kidneys. Unlike in our previous study in mice [14], we observed only moderate tracer uptake in the pancreas. The estimated effective doses are similar to those of other ^{18}F-labeled radioligands [21].

Neuroendocrine tumors showed an initial uptake followed by washout, consistent with lack of trapping within the tumors. In contrast, the gliomas showed excellent ^{18}F-FETrp tracer uptake with prolonged accumulation in the presence of very low uptake in non-tumoral brain. In addition, high ^{18}F-FETrp uptake provided differential spatial information with respect to tracer accumulation within a larger tumor mass, rendering ^{18}F-FETrp a promising tracer to identify tumor regions for treatment targeting. Similar to previous PET studies with AMT and other amino acid analog radiotracers, ^{18}F-FETrp may detect non-enhancing glioma portions and differentiate contrast-enhanced tumor regions from non-tumoral mass

(such as edema) [7–9]. However, the potential ability of ^{18}F-FETrp uptake to reflect IDO activity and respond to IDO inhibition sets it apart from other ^{18}F-labeled amino acid PET tracers. Since KP activation contributes to an immunosuppressive tumor microenvironment, associated with malignant phenotype and poor prognosis [16, 22], the KP is an attractive target for glioma immunotherapy. Pending further studies, ^{18}F-FETrp-PET holds the promise to serve as a unique molecular imaging approach to study tryptophan metabolism *in vivo*.

Conclusion

Our study provides strong proof-of-principle data for the potential clinical value of ^{18}F-FETrp-PET for molecular imaging of human gliomas.

Declarations

ACKNOWLEDGEMENT

We are grateful to Hancheng Cai, PhD, PET Radiochemistry Facility, Department of Radiology, Mayo Clinic, Jacksonville, Florida, for his input regarding radiochemistry.

DISCLOSURE

The study was supported by the Karmanos Cancer Institute SRIG and the National Cancer Institute (P30CA022453). No other potential conflict of interest relevant to this article was reported.

AUTHOR CONTRIBUTIONS

We declare that all authors made a substantial contribution to this manuscript.

References

1. Comai S, Bertazzo A, Brughera M, Crotti S (2020) Tryptophan in health and disease. Adv Clin Chem 95:165–218
2. Munn DH, Mellor AL (2013) Indoleamine 2,3 dioxygenase and metabolic control of immune responses. Trends Immunol 34(3):137–143
3. Wainwright DA, Balyasnikova IV, Chang AL et al (2012) IDO expression in brain tumors increases the recruitment of regulatory T cells and negatively impacts survival. Clin Cancer Res 18(22):6110–6121
4. Ala M (2021) The footprint of kynurenine pathway in every cancer: a new target for chemotherapy. Eur J Pharmacol 896:173921
5. Juhász C, Chugani DC, Muzik O et al (2006) In vivo uptake and metabolism of alpha-[^{11}C]methyl-L-tryptophan in human brain tumors. J Cereb Blood Flow Metab 26:345–357

6. Batista CEA, Juhász C, Muzik O et al (2009) Imaging correlates of differential expression of indoleamine 2,3-dioxygenase in human brain tumors. Mol Imaging Biol 11:460–466
7. Alkonyi B, Barger GR, Mittal S et al (2012) Accurate identification of recurrent gliomas from radiation injury by kinetic analysis of alpha-[^{11}C]methyl-L-tryptophan PET. J Nucl Med 53:1058–1064
8. Juhász C, Dwivedi S, Kamson DO, Michelhaugh SK, Mittal S (2014) Comparison of amino acid positron emission tomography radiotracers for molecular imaging of primary and metastatic brain tumors. Mol Imaging 13. 10.2310/7290.2014.00015
9. John F, Bosnyak E, Robinette NL et al (2019) Multimodal imaging-defined subregions in newly-diagnosed glioblastoma: Impact on overall survival. Neuro Oncol 21:264–273
10. Chugani DC, Muzik O (2000) Alpha[C-11]methyl-L-tryptophan PET maps brain serotonin synthesis and kynurenine pathway metabolism. J Cereb Blood Flow Metab 20(1):2–9
11. Henrottin J, Lemaire C, Egrise D et al (2016) Fully automated radiosynthesis of N1-[(^{18}F)]fluoroethyl-tryptophan and study of its biological activity as a new potential substrate for indoleamine 2,3-dioxygenase PET imaging. Nucl Med Biol 43:379–389
12. Xin Y, Cai H (2017) Improved Radiosynthesis and biological evaluations of L- and D-1-[^{18}F]fluoroethyl-tryptophan for PET imaging of IDO-mediated kynurenine pathway of tryptophan metabolism. Mol Imaging Biol 19:589–598
13. Xin Y, Gao X, Liu L, Ge WP, Jain MK, Cai H (2019) Evaluation of L-1-[^{18}F]fluoroethyl-tryptophan for PET imaging of Cancer. Mol Imaging Biol 21:1138–1146
14. Michelhaugh SK, Muzik O, Guastella AR et al (2017) Assessment of tryptophan uptake and kinetics using 1-(2-[^{18}F]fluoroethyl)-L-tryptophan and α-[^{11}C]-methyl-L-tryptophan PET imaging in mice implanted with patient-derived brain tumor xenografts. J Nucl Med 58:208–213
15. John F, Muzik O, Mittal S, Juhász C (2020) Fluorine-18-labeled PET radiotracers for imaging tryptophan uptake and metabolism: A systematic review. Mol Imaging Biol 22:805–819
16. Mitsuka K, Kawataki T, Satoh E, Asahara T, Horikoshi T, Kinouchi H (2013) Expression of indoleamine 2,3-dioxygenase and correlation with pathological malignancy in gliomas. Neurosurgery 72(6):1031–1038
17. Jiang H, Guo Y, Cai H et al (2023) Automated radiosynthesis of 1-(2-[^{18}F]fluoroethyl)-L-tryptophan ([^{18}F]FETrp) for positron emission tomography (PET) imaging of cancer in humans. J Label Comp Radiopharm 66(7–8):180–188
18. Shiyam Sundar LK, Yu J, Muzik O et al (2022) Fully Automated, Semantic Segmentation of Whole-Body ^{18}F-FDG PET/CT Images Based on Data-Centric Artificial Intelligence. J Nucl Med 63(12):1941–1948
19. Stabin MG (1996) MIRDOSE: personal computer software for internal dose assessment in nuclear medicine. J Nucl Med 37:538–546
20. Stabin MG, Siegel JA (2003) Physical models and dose factors for use in internal dose assessment. Health Phys 85:294–310

21. Quinn B, Dauer Z, Pandit-Taskar N, Schoder H, Dauer LT (2016) Radiation dosimetry of ^{18}F-FDG PET/CT: incorporating exam-specific parameters in dose estimates. BMC Med Imaging 16:41
22. Platten M, Friedrich M, Wainwright DA, Panitz V, Opitz CA (2021) Tryptophan metabolism in brain tumors - IDO and beyond. Curr Opin Immunol 70:57–66

Tables

Tables 1-2 is available in the Supplementary Files section.

Figures

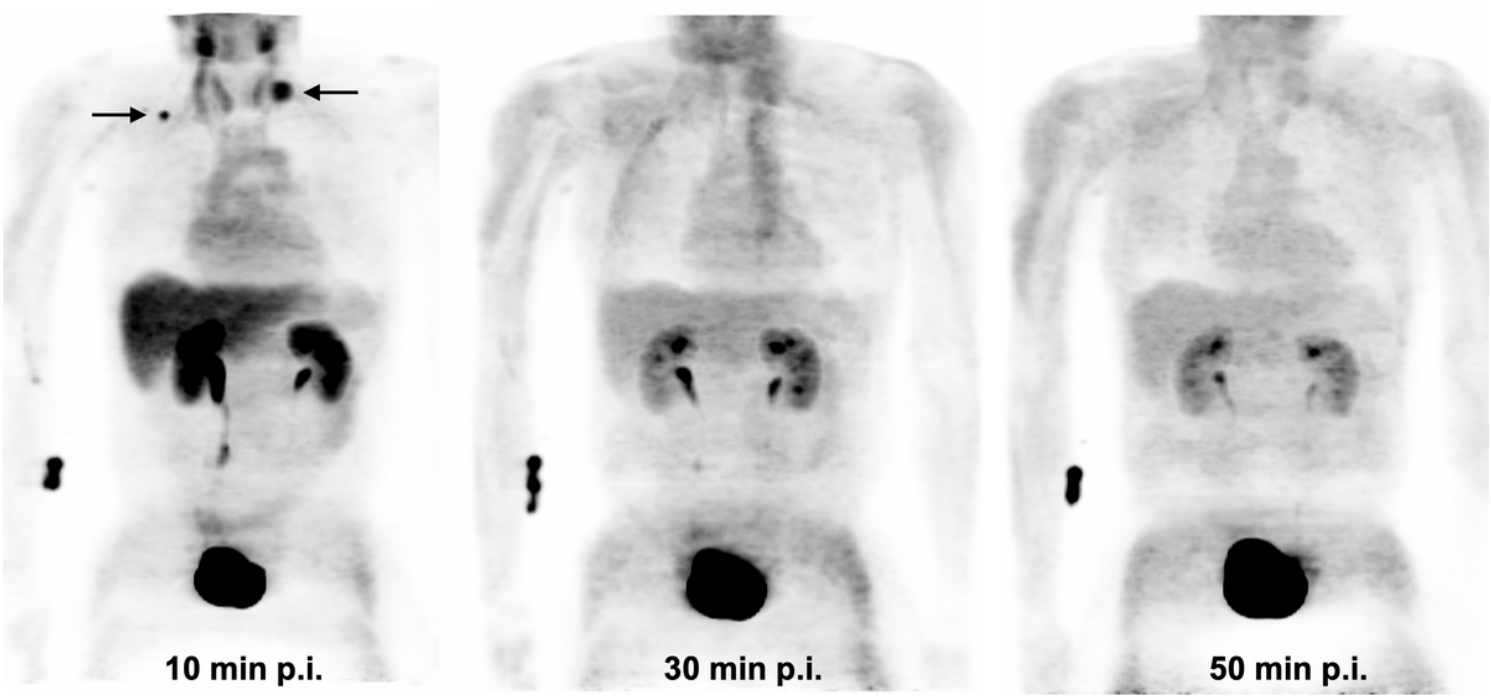

Figure 1

Maximum intensity projection images of a male patient with neuroendocrine tumors (arrows) at 10, 30, and 50-min after ^{18}F-FETrp injection. The images showed initial uptake in the kidneys, liver, and tumor tissue (arrows), with subsequent tracer extraction via urine resulting in high tracer accumulation in the bladder.

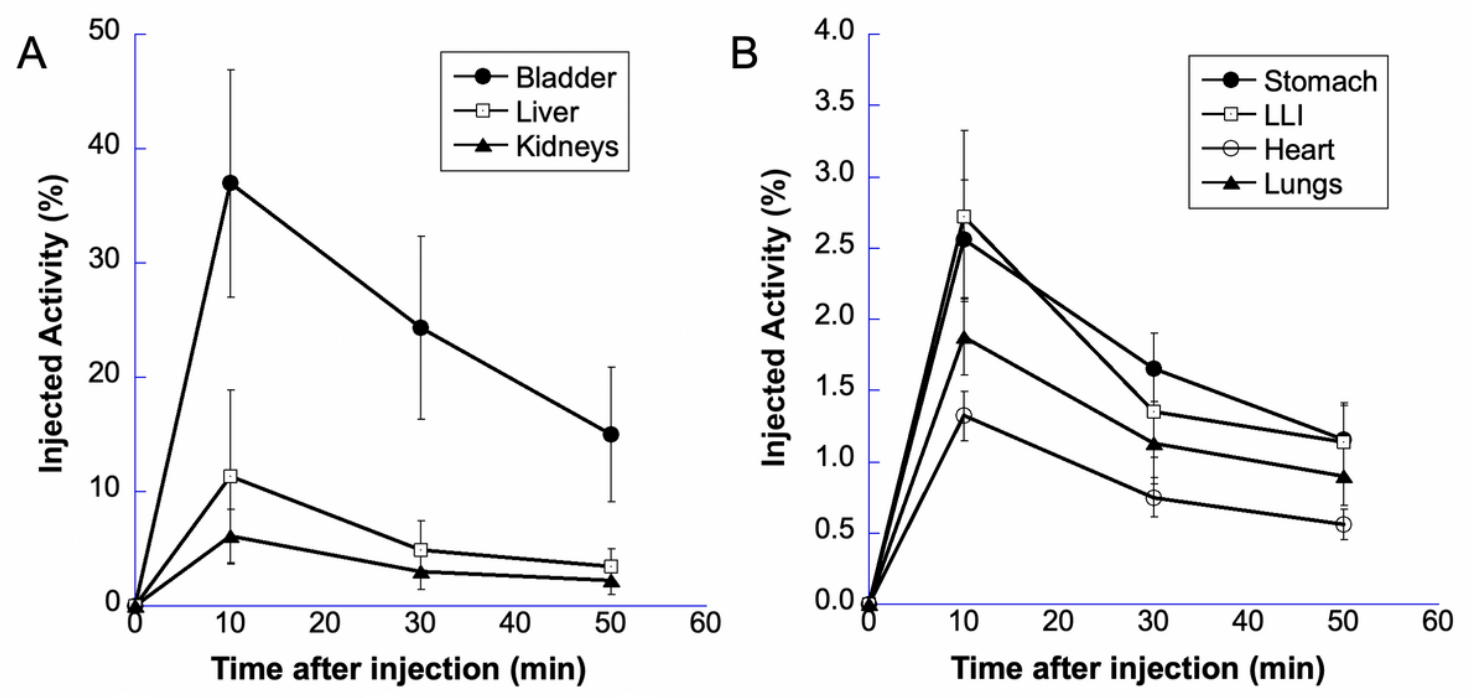

Figure 2

Mean radioactivity from ^{18}F-FETrp in various organs. A fast initial organ uptake is followed by steady washout. Data are mean ± SD in four subjects. LLI=lower large intestines

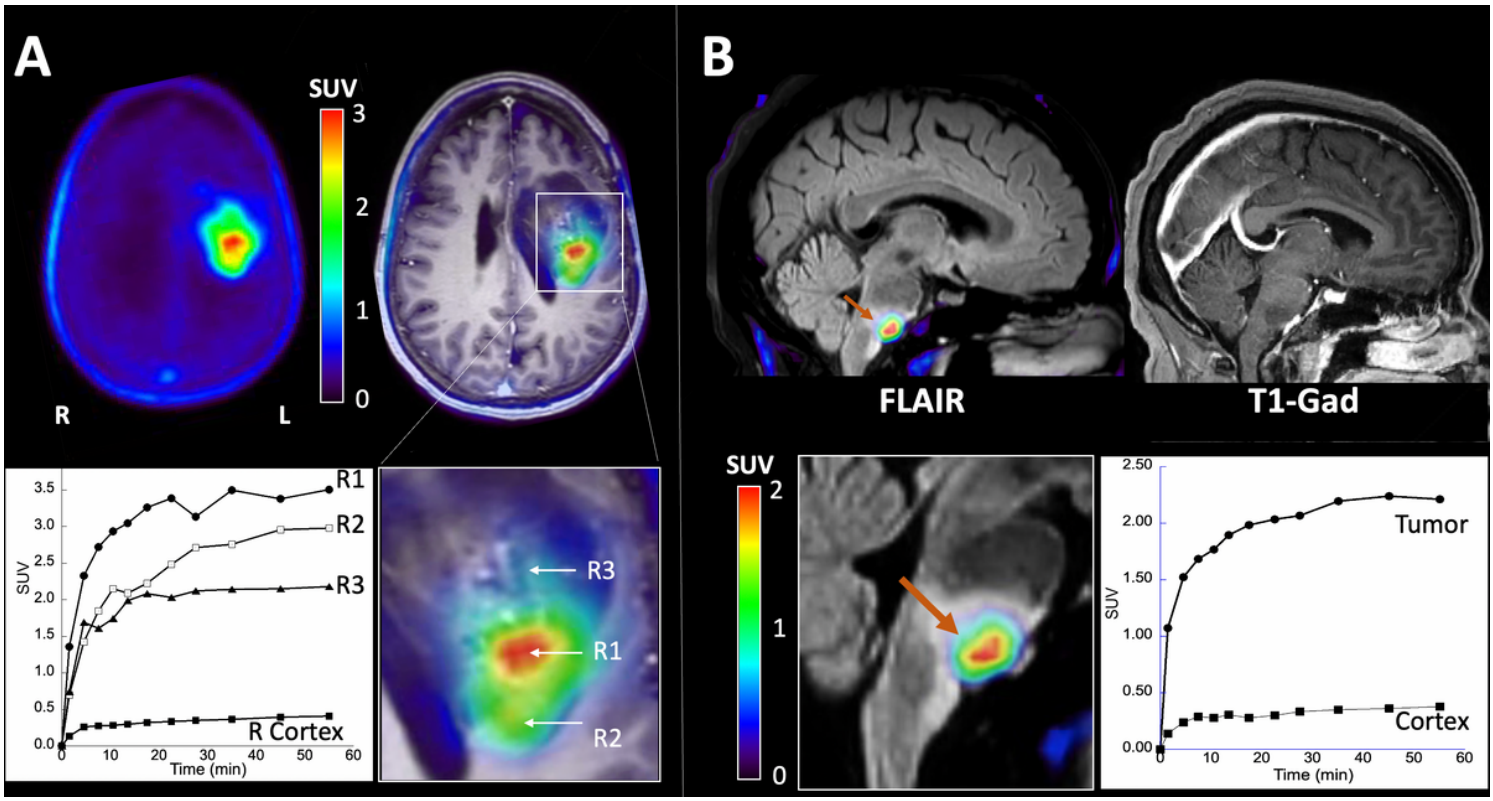

Figure 3

Uptake of ^{18}F-FETrp in two patients with a glioma. (**A**) Heterogeneous tracer accumulation in a left hemispheric contrast-enhancing tumor mass in a 64-year-old woman, who had a history of a resection of a low-grade glioma; recent MRIs suggested slow tumor progression behind the previous resection cavity. The images (summed uptake 40-60 min p.i.) clearly identified a portion of the MRI-detected mass with high, sustained tracer accumulation (R1) in addition to a posterior "warm" region (R2) and fairly large portion that showed lower tracer uptake (R3). (**B**) ^{18}F-FETrp accumulation in a slowly growing brainstem mass in a 37-year-old woman; high uptake was confined to the anterior portion of the FLAIR-hyperintense, non-contrast-enhancing area. Biopsy obtained from this area showed a diffuse astrocytoma. For both tumors, the corresponding time-activity curves indicated trapping of tracer in tumor tissue, resulting in excellent contrast of all the tumor regions against normal brain tissue.

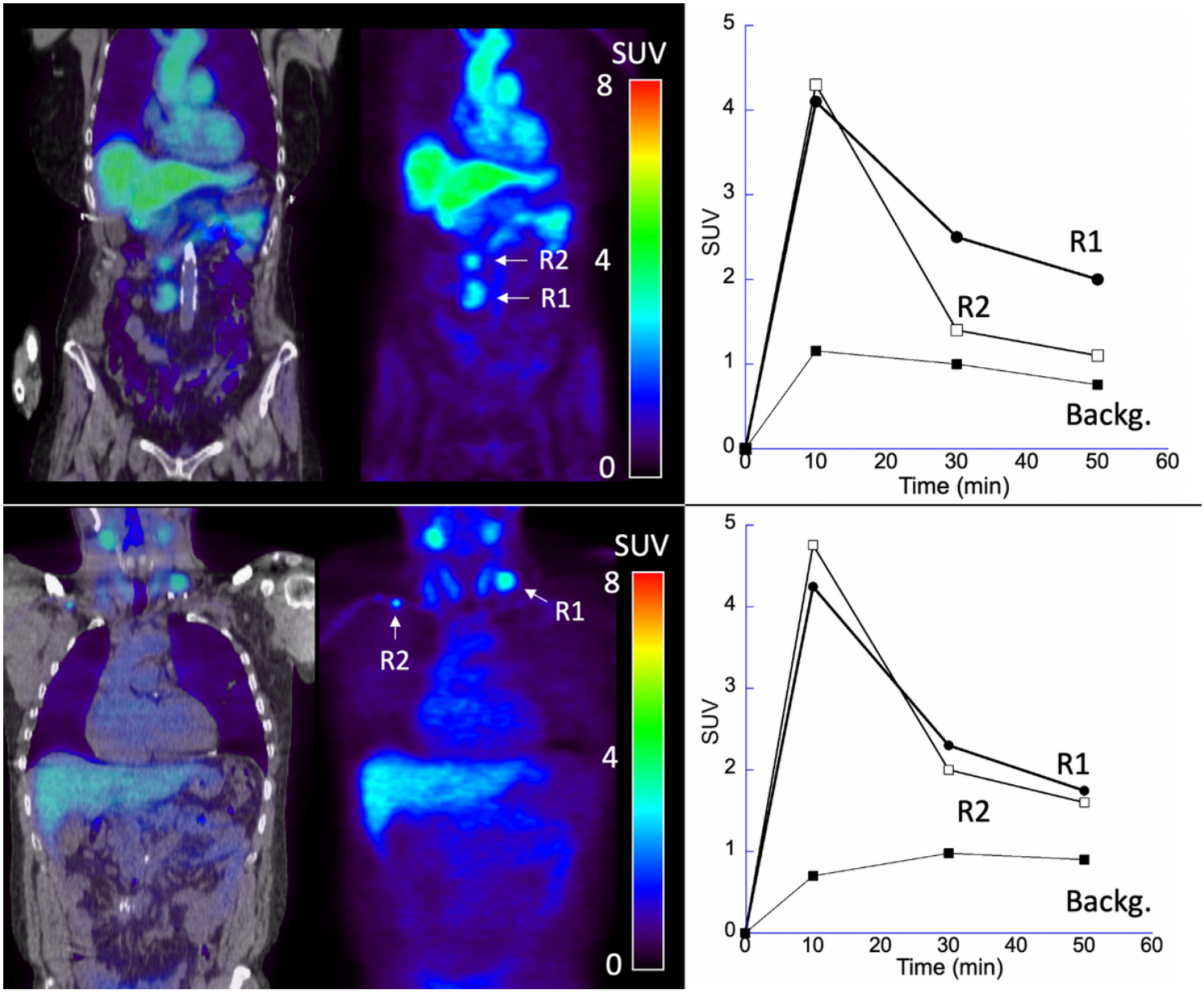

Figure 4

^{18}F-FETrp Uptake in two patients with neuroendocrine tumors (arrows; 10-min post-injection). In contrast to the uptake in brain tumors, the tracer underwent washout following high initial uptake (at 10-min p.i.).

Supplementary Files

This is a list of supplementary files associated with this preprint. Click to download.

- Table12.docx
- SUPPLEMENTALDATAFETrp.docx